sciendo

ISSN 1335-8871

MEASUREMENT SCIENCE REVIEW

Journal homepage: https://content.sciendo.com

Signal Smoothing with Time-Space Fractional Order Model

Yuanlu Li[1,2]

[1] *Jiangsu Collaborative Innovation Center of Atmospheric Environment and Equipment Technology (CICAEET), Nanjing University of Information Science & Technology, No.219 Ningliu Road, 210044, Nanjing, China, lyl_nuist@nuist.edu.cn*
[2] *School of Automation, Nanjing University of Information Science & Technology, No.219 Ningliu Road, 210044, Nanjing, China*

The time-space fractional-order model (TSFOM) is a generation of the classical diffusion model which is an excellent smoothing method. In this paper, the fractional-order derivative in the model is found to have good performance for peak-preserving. To check the validity and performance of the model, some noisy signals are smoothed by some commonly used smoothing methods and results are compared with those of the proposed model. The comparison result shows that the proposed method outperforms the classical nonlinear diffusion model and some commonly used smoothing methods.

Keywords: Fractional diffusion, signal smoothing, filtering.

1. INTRODUCTION

With the development of fractional calculus, a new set of tools was developed by replacing calculus in classic procedures and implementations with the fractional order calculus [1]-[3]. In this paper, a time-space fractional-order model, improved from the classical nonlinear diffusion model [4], was suggested as a smoothing tool.

The application of diffusion equations to signal processing can be traced back to the year 1983 [5]. Since then, it has been widely concerned to apply diffusion filtering to signal signals. However, the homogeneous linear diffusion filtering does not take into account the characteristic information of a signal, such as a peak while suppressing noise, it also blurs features of a signal. Fortunately, the problem has been solved by a nonlinear isotropic diffusion filtering suggested by Perona and Malik [6]. So, nonlinear diffusion filtering has been widely used in image processing [7]-[18]. An overview of the diffusion filtering was given by Weickert [19].

It is a challenge to smooth a noisy signal for preserving features such as peak or discontinuity. Therefore, some research has been focused on features preservation [4], [8], [11], [20], [21]. For instance, nonlinear diffusion filtering was designed to smooth spectrum data while preserving peaks [4]. In image processing, nonlinear diffusion filtering, total variation model, etc. were widely used for features-preserving filtering [8], [11], [20], [21]. Among these methods, the features of a signal can be preserved having the feedback in the iterative process. In recent years, some fractional models were proposed to improve some classical models. For example, the spatial-fractional order model was used for signal smoothing [22], the time-fractional model was suggested to smooth noisy signals [23], [24], the generalized fractional time integral was proposed for image denoising [3], the fractional-order model was explored to denoise image [26], and a fully fractional anisotropic diffusion model was introduced to denoise image [27].

The space-time fractional diffusion equation has been suggested for models of the anomalous diffusion [28], where particle sticking and trapping phenomena can be described with the time fractional derivative, and long particle jumps can be modeled by the fractional space derivative. For more background of the time-space fractional diffusion model, please refer to [29], [30].

There are very few papers about the application of the time-space fractional-order model to signal smoothing. However, it should be suitable for signal smoothing. The reasons are as follows: The classical nonlinear diffusion filtering can preserve important features of a signal such as peaks [4] and edges [8], [20]. Furthermore, the derivative can be used as a tool to enhance some details of a signal [31] or an image [32]. The fractional derivative of a signal or an image is equivalent to $\frac{\partial^{\alpha} u(x,t)}{\partial x^{\alpha}}$ which can be viewed as the right side of the time-space fractional order model. Besides, the left side of the time-space fractional order

DOI: 10.2478/msr-2021-0004

model $\dfrac{\partial^{\alpha}u(x,t_k)}{\partial t^{\alpha}}$ is a weighted sum of $u(x,t_i)$ for $i=0,1,\cdots,k$.

To preserve the peaks of the signal, it is necessary to design a suitable diffusion function. A natural idea is that the diffusion strength is weakened as the peak height increases. So $K\left[\left|u(x,t)\right|\right]=\exp\left[-\left(\dfrac{\left|u(x,t)\right|}{\lambda}\right)^2\right]$ is a good choice for diffusion functions, where $\left|u(x,t)\right|$ is taken as an indicator of the peak in a signal, one can find that the bigger $\left|u(x,t)\right|$ is, the smaller $K\left[\left|u(x,t)\right|\right]$ is for a fixed λ. So, the time-space fractional order model is proposed.

Some simulated spectra are generated to compare the proposed model with the classical nonlinear model and other smoothing methods including the Savitzky-Golay smoothing method [33], [34], the regularization method is proposed based on penalized least squares [35], [36], the nonparametric smoothing method [37], and the wavelet denoised method [38], [39]. Finally, the time-space fractional-order model is applied to the smoothing of an NMR spectrum of wood [35].

2. TIME-SPACE FRACTIONAL-ORDER MODEL

This model is obtained by extending the classical diffusion model, which means that the time derivative term on the left side of the equation is substituted by the Caputo fractional derivative of order, and the space derivatives term on the right side is substituted by the Riesz fractional derivatives of order β, respectively. The proposed model is given as follows

$$\frac{\partial^{\alpha}u(x,t)}{\partial t^{\alpha}}=g\left[\left|u(x,t)\right|\right]\frac{\partial^{\beta}u(x,t)}{\partial x^{\beta}},\quad \alpha\in(1,1.3),2<\beta<3\cdots(1)$$

where $\dfrac{\partial^{\beta}}{\partial x^{\beta}}$ is the fractional-order Riesz derivative, $g\left[\left|u(x,t)\right|\right]$ is the diffusion function.

There are some numerical methods for the time-space fractional diffusion model; in this subsection, we shall consider the finite difference scheme by which finite difference is easily handled and digital signals are already discrete [40]-[44].

2.1. Discretization of the proposed model

The Caputo fractional order derivative is shown as

$$\frac{\partial^{\alpha}u(x,t)}{\partial t^{\alpha}}=\frac{1}{\Gamma(2-\alpha)}\int_0^t\frac{\partial^2u(x,\xi)}{\partial\xi^2}\frac{1}{(t-\xi)^{\alpha-1}}d\xi,\quad 1<\alpha<2 \tag{2}$$

which can be approximated by [34]

$$\frac{\partial^{\alpha}u_i^k}{\partial t^{\alpha}}\cong\frac{\tau^{-\alpha}}{\Gamma(3-\alpha)}\left[\left(u_i^k-u_i^{k-1}\right)+\sum_{j=2}^{k}\left(\omega_j^{(\alpha)}-\omega_{j-1}^{(\alpha)}\right)\left(u_i^{k-j+1}-u_i^{k-j}\right)\right] \tag{3}$$

where

$$\omega_j^{(\alpha)}=j^{2-\alpha}-(j-1)^{2-\alpha}, \tag{4}$$

and $1=\omega_1^{(\alpha)}>\omega_2^{(\alpha)}>\cdots>\omega_k^{(\alpha)}$.

2.2. Computation of symmetric Riesz derivatives

The symmetric Riesz derivatives of order β can be obtained by equation (5)

$$\left[f_N^{(\beta)}\quad\cdots\quad f_1^{(\beta)}\quad f_0^{(\beta)}\right]^T=R_N^{(\beta)}\left[f_N\quad\cdots\quad f_1\quad f_0\right]^T \tag{5}$$

where $f_n^{(\beta)}$, $1,2,\cdots,N$ represents the β order Riesz derivative,

$$R_N^{(\beta)}=\frac{1}{h^{-\beta}}\begin{bmatrix}\mu_0^{(\beta)} & \mu_1^{(\beta)} & \mu_2^{(\beta)} & \mu_3^{(\beta)} & \cdots & \mu_N^{(\beta)}\\ \mu_1^{(\beta)} & \mu_0^{(\beta)} & \mu_1^{(\beta)} & \mu_2^{(\beta)} & \cdots & \mu_{N-1}^{(\beta)}\\ \mu_2^{(\beta)} & \mu_1^{(\beta)} & \mu_0^{(\beta)} & \mu_1^{(\beta)} & \cdots & \mu_{N-2}^{(\beta)}\\ \ddots & \ddots & \ddots & \ddots & \cdots & \cdots\\ \mu_{N-1}^{(\beta)} & \ddots & \mu_2^{(\beta)} & \mu_1^{(\beta)} & \mu_0^{(\beta)} & \mu_1^{(\beta)}\\ \mu_N^{(\beta)} & \mu_{N-1}^{(\beta)} & \ddots & \mu_2^{(\beta)} & \mu_1^{(\beta)} & \mu_0^{(\beta)}\end{bmatrix} \tag{6}$$

$$\mu_m^{(\beta)}=\frac{(-1)^k\Gamma(\beta+1)\cos(\beta\pi/2)}{\Gamma(\beta/2-k+1)\Gamma(\beta/2+k+1)}, \tag{7}$$

where $k=0,1,\cdots,N$.

2.3. Iterative scheme

According to the implicit difference scheme, the iterative scheme is as follows

$$U^1=A^{-1}U^0 \tag{8}$$

where $A=I-\Gamma(3-\alpha)\tau^{\alpha}GR_N^{(\beta)}$, I is an identity matrix, $G=\begin{bmatrix}g_0^{i-1} & & & \\ & g_1^{i-1} & & \\ & & \ddots & \\ & & & g_N^{i-1}\end{bmatrix}$, $U^i=\begin{bmatrix}u_0^i\\ u_1^i\\ \vdots\\ u_N^i\end{bmatrix}$.

$$U^i=A^{-1}B\ \text{ for}\, i\geq 2. \tag{9}$$

where $B=U^{i-1}-\sum_{j=2}^{i}\left(\omega_j^{(\alpha)}-\omega_{j-1}^{(\alpha)}\right)\left(U^{i-j+1}-U^{i-j}\right)$.

3. SIMULATED DATA AND SMOOTHING PERFORMANCE INDEX

The Lorentzian-shaped peak is commonly taken as a model for the spectral peak. Therefore, the Lorentzian-shaped peaks here are taken to test the proposed method, it is generated by

$$L(x)=\sum_{i=1}^{n}\frac{A_i}{1+\left(\frac{x-\mu_i}{\sigma_i}\right)^2} \tag{10}$$

In $L(x)$, the number of peaks is n, the height, position, and width are A_i, μ_i, and σ_i, respectively. The noise is added by the "awgn" function.

In general, the filtering performance is measured by the signal-to-noise ratio. The higher the signal-to-noise ratio of the filtered signal, the better the filtering performance. The signal-to-noise ratio formula is as follows.

$$SNR=10\log\frac{\sum_{n=0}^{N-1}s^2(n)}{\sum_{n=0}^{N-1}|f(n)-s(n)|^2} \tag{11}$$

where $s(n)$ is a noise-free signal and $f(n)$ is a noisy signal. Here, it will be taken as a smoothing performance index.

Another measurement is root mean square error (RMSE), which is given by

$$RSME=\sqrt{\frac{1}{N}\sum_{n=0}^{N-1}[f(n)-s(n)]^2} \tag{12}$$

4. RESULTS AND DISCUSSION

In the proposed model, there are four parameters: fractional time derivative order α , space fractional derivative order β , time-step size τ , and the iteration number k . The fractional time derivative order α is between 1.0 and 1.2, usually α can be set as 1.1. Space fractional derivative order β is between 2 and 2.95, usually, it can be set as 2.75. If you want to preserve the peak shape of a signal, space fractional derivative order should be big. The time step size τ can be fixed as 1.

4.1. Effect of the diffusion function on smoothing

Shortcoming of the Gaussian smoothing is that it removes the noise of a signal while distorting the peak. Therefore, one natural idea is to control the diffusion process by the diffusion function. If some parts of a signal, such as a peak, need to be preserved, corresponding values of the diffusion function approach zero. Conversely, the values of the diffusion function should be big. Here, the diffusion function is designed using the signal to be smoothed as a reference signal, and the formula is as follows

$$g\left[|u(x,t_k)|\right]=\exp\left[-\left(\frac{|u(x,t_{k-1})|}{\lambda(t_k)}\right)^2\right] \tag{13}$$

One can easily find that the range of $g\left[|u(x,t)|\right]$ is from 0 to 1, and the bigger $|u(x,t)|$, the smaller $g\left[|u(x,t)|\right]$, for an appropriate λ . So, the peak can be preserved well in the smoothing process. Usually, parameter λ can be determined by the expected diffusion strength. For example, if one expects the diffusion strength at the peak to be 0.05, then $\lambda(t_k)$ can be obtained by

$$\lambda(t_k)=\frac{\max(u(x,t_{k-1}))}{\sqrt{-\ln(0.05)}} \tag{14}$$

Of course, if you want the diffusion strength at the peak to be 0.2, $\lambda(t_k)$ should be changed as follows,

$$\lambda(t_k)=\frac{\max(u(x,t_{k-1}))}{\sqrt{-\ln(0.2)}} \tag{15}$$

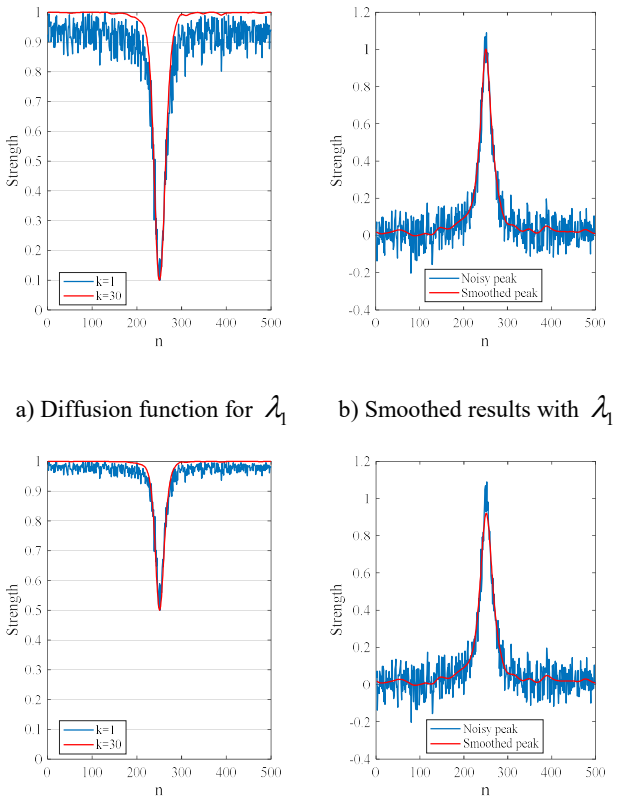

a) Diffusion function for λ_1 b) Smoothed results with λ_1

c) Diffusion function for λ_2 d) Smoothed results with λ_2

Fig.1. A noisy peak and its smoothed result with different λ .

As an example, a noisy Gaussian-shaped peak marked with Noisy peak in Fig.1.b) is taken to observe the effect of λ in the diffusion process.

Fig.1.a) and Fig.1.c) shows the diffusion functions at different iteration numbers 1 and 30, respectively. After 30 iterations, the smoothed signals are shown in Fig.1.b) and Fig.1.d) with the red line. Their diffusion strength at the highest peak is 0.1 and 0.5, respectively.

One easily finds that the larger λ, the stronger the diffusion, which will also result in the peak height decrease.

4.2. Comparison and performance evaluation of the TSFOM

Different methods were developed for finding smooth signals. Thus, in order to compare the TSFOM with the classical diffusion model (CDM) ($\alpha = 1$, $\beta = 2$), regularization method (RegM), wavelet method (WM), nonparametric smoothing method (Non-P), and the Savitzky-Golay method (SGM) were used. Four signals with white noise are generated, the SNR is 10 dB, 15 dB, 20 dB, and 25 dB, respectively. The smoothed results obtained by the TSFOM are shown in Fig.2. where they are marked with "Smoothed signal".

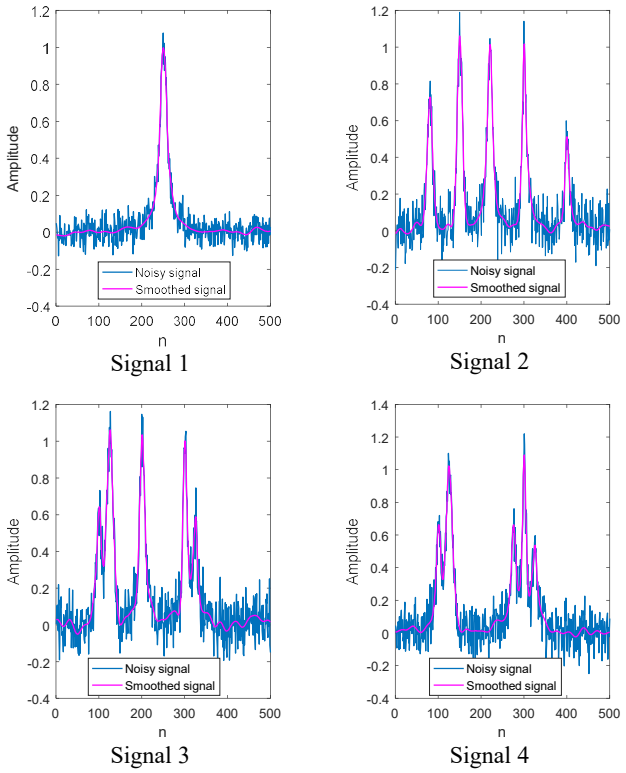

Fig.2. Noisy signals (10dB) and smoothed results of the TSFOM.

One purpose of smoothing is to suppress noise and improve the SNR of a signal. Therefore, the SNR of the optimal results for each method is presented in Table 1.

In addition, the root mean square errors of the optimal results are also computed and shown in Fig.3. The RMSE of the TSFOM is the smallest.

Fig.3. shows that the results obtained by the proposed model are superior to CDM, WM, SGM, Non-P, and RegM.

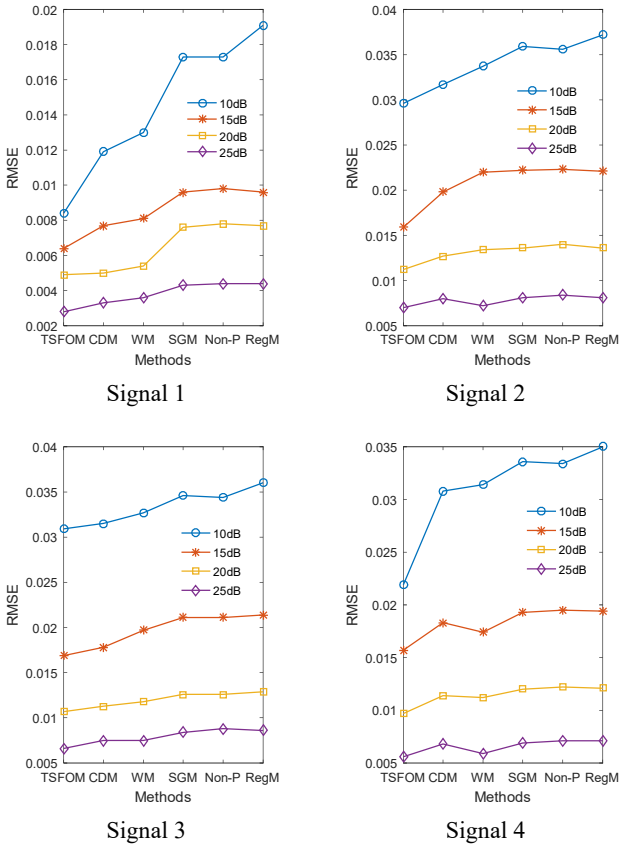

Fig.3. RMSE comparison of different methods.

Table 1. SNR improvement for different smoothing methods.

Signal	SNR (dB)	TSFOM	CDM	WM	SGM	Non_P	RegM
1	10	26.47	23.47	22.72	20.19	20.20	19.33
	15	28.80	27.91	26.76	25.32	25.16	25.29
	20	31.14	30.97	30.27	27.30	27.07	27.24
	25	36.16	34.50	33.79	32.27	32.01	32.10
2	10	19.33	18.73	18.21	17.67	17.73	17.35
	15	24.08	22.84	21.91	21.85	21.81	21.88
	20	27.79	26.67	26.21	26.09	25.84	26.07
	25	31.91	30.73	31.68	30.60	30.27	30.55
3	10	19.47	19.38	18.98	18.51	18.55	18.15
	15	24.71	24.28	23.37	22.81	22.80	22.67
	20	28.69	28.21	27.81	27.29	27.24	27.09
	25	32.89	31.82	31.77	30.78	30.39	30.57
4	10	21.88	18.92	18.75	18.16	18.20	17.80
	15	24.78	23.45	23.89	22.98	22.90	22.94
	20	28.94	27.58	27.69	27.12	26.95	27.02
	25	33.67	32.00	33.23	31.92	31.63	31.70

4.3. Preserving peak performance

Usually, the peak height of the smoothed signal decreases and the peak width of the smoothed signal become wider. Therefore, peak-preserving smoothing is a challenging task. The Savitzky-Golay method, wavelet method, nonparametric smoothing method, regularization method, and the classical nonlinear diffusion method are some smoothing methods that can preserve peaks of the raw signal. So, these methods are used for comparing the TSFOM. For this purpose, around each peak, nine points are selected to fit the peak shape and the peak shape parameters are obtained, they are the peak position, the peak height, and the peak width. Thus, their errors for each peak can be easily obtained. Their average error for each signal is presented in Fig.4., which shows that the TSFOM and CDM are effective at preserving peak shape.

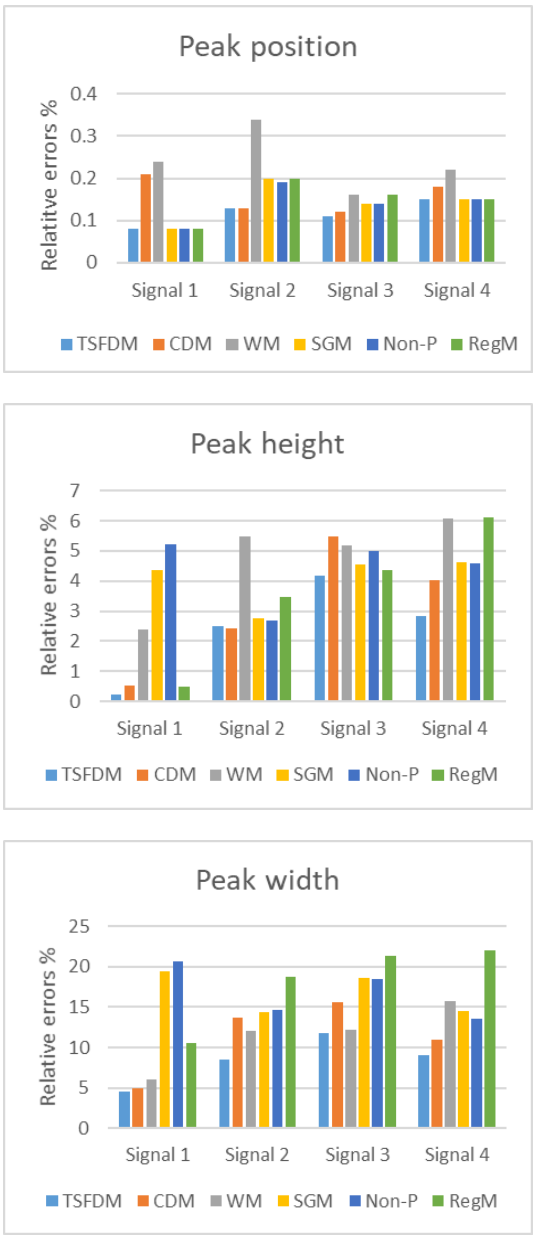

Fig.4. Relative errors of peak shape parameters.

4.4. The best iteration number

The "two-fold" cross-validation is used for a purposive choice of iteration number. Firstly, the proposed model was used to obtain the smoothed signal of the odd-indexed down-samples. Then the smoothed signal was interpolated to get the full signal. The relationship between the standard deviation (SD) and the iteration number is shown in Fig.5. The best iteration number can be determined by the minimal value of the standard deviation (SD) of the even-indexed down-samples.

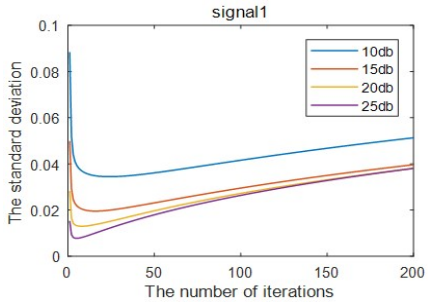

a) Signal 1

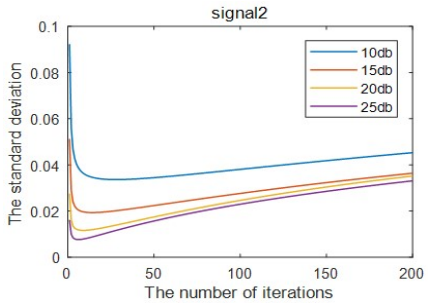

b) Signal 2

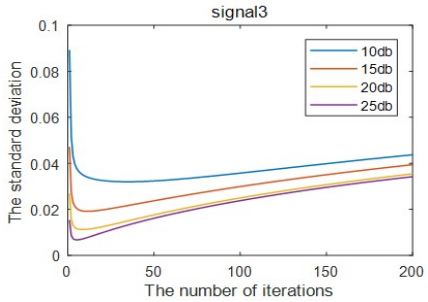

c) Signal 3

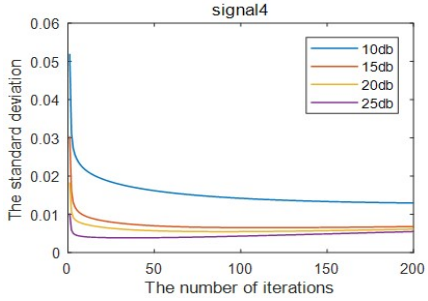

d) Signal 4

Fig.5. The variation of standard deviation with the number of iterations, the lower the SNR is, the more iterations are required to achieve the best smoothing performance.

5. APPLICATION OF THE PROPOSED MODEL

5.1. Application of the proposed model in the NMR spectrum

The TSFOM is applied to smooth the NMR spectrum and compares with the regularization method [35], [36] and the wavelet denoised method [39]. The smoothed results obtained by the TSFOM are shown in Fig.6. The signal is from [35], in which it was filtered by the regularization method. For the regularization method, the optimal result is directly obtained with the codes in [35].

For the wavelet denoised method, the smoothing result is obtained by the function "wden" in the Wavelet toolbox whit Donoho and Johnstone's universal threshold at level 6 by the sym8 wavelet. For the TSFOM, the time step size is set to 1, the time fractional-order derivative is 1.05 and the space fractional-order derivative is 2.95. The result for 40 iterations is shown in Fig.6.d). The highest peak of the raw NMR spectrum and smoothed result obtained by different methods are given in Table 2.

Fig.6. and Table 2. show the regularization method is more effective at preserving peaks but less effective at reducing noise. The wavelet denoised method has a better effect on noise reduction, but the peaks are obviously weakened. However, the TSFOM is not only effective at denoising noise, but also effective at preserving peaks of the NMR spectrum.

Table 2. The highest peak of the raw spectrum and the smoothed signal.

	Raw spectrum	TSFOM	WM	RegM
Height	58.02	57.30	48.74	52.67

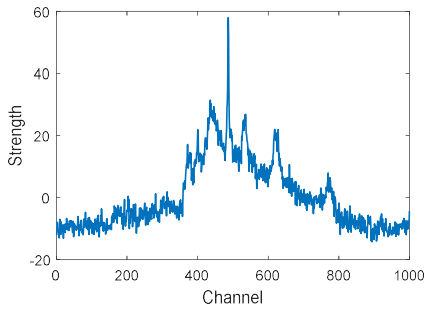

a)Raw NMR spectrum

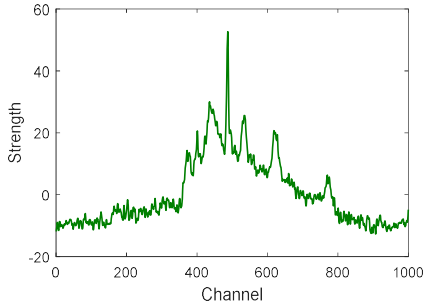

b) The smoothed result obtained by RegM

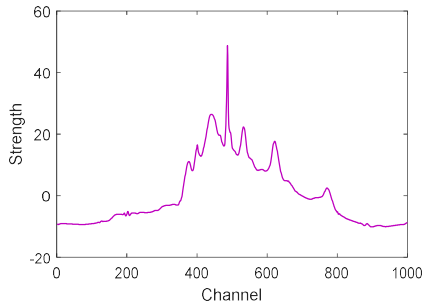

c) The smoothed result obtained by WM

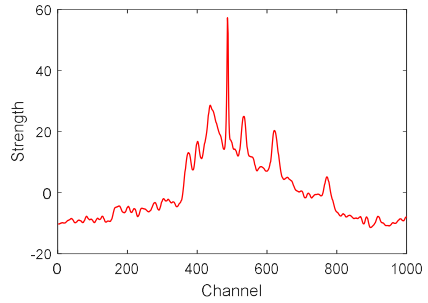

d) The smoothed result obtained by TSFOM

Fig.6. The TSFOM is used to smooth the NMR spectrum.

5.2. Smoothing of the mass spectra

One of the challenges for the mass spectra smoothing is peak preserving. The mssgolay is suggested to smooth the raw mass spectra in the Bioinformatics Toolbox™. The comparison results are shown in Fig.7. One can find that the proposed model has better peak-preserving capability at a fairly smooth level of the polynomial filter.

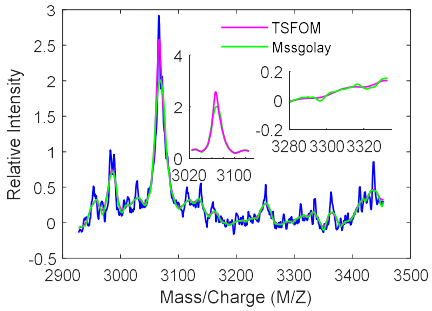

a) The smoothing result for mspec01

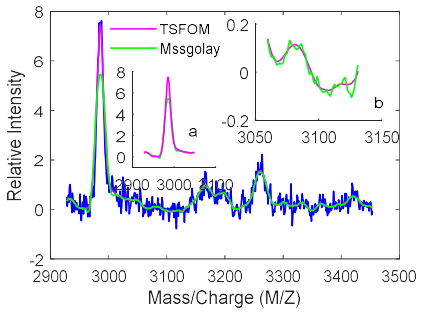

b) The smoothing result for mspec03

Fig.7. Smoothing of the mass spectra with the TSFOM.

6. CONCLUSION

A time-space fractional diffusion model is obtained by extending the classical nonlinear diffusion model. The corresponding numerical algorithm and parameter setting method were given. The proposed method was verified by some simulated signals and real signals. The TSFOM is not only effective at suppressing noise, but also effective at preserving peak. The principle of peak-preserving smoothing of time-space fractional order model is still an open problem.

ACKNOWLEDGMENTS

The work was partly supported by the National Natural Science Foundation of China (Grant: 61671010), the Natural Science Foundation of Jiangsu Province of China (Grant: BK20161535) and Qing Lan Project of Jiangsu Province (Grant: B2018Q03).

REFERENCES

[1] Mathieu, B., Melchior, P., Oustaloup, A., Ceyral, C. (2003). Fractional differentiation for edge detection. *Signal Processing*, 83 (11), 2421-2432.

[2] Cuesta, E., Kirane, M., Malik, S.A. (2012). Image structure preserving denoising using generalized fractional time integrals. *Signal Processing*, 92 (2), 553-563.

[3] Magin, R., Ortigueira, M.D., Podlubny, I., Trujillo, J. (2011). On the fractional signals and systems. *Signal Processing*, 91 (3), 350-371.

[4] Li, Y.L., Ding, Y.Q., Li, T. (2016). Nonlinear diffusion filtering for peak-preserving smoothing of a spectrum signal. *Chemometrics and Intelligent Laboratory Systems,* 156, 157-165.

[5] Witkin, A.P. (1983). Scale-space filtering. In *Proceedings of the Eighth International Joint Conference on Artificial Intelligence, Volume 2*. Morgan Kaufmann Publishers, 1019-1022.

[6] Perona, P., Malik, J. (1990). Scale-space and edge detection using anisotropic diffusion. *IEEE Transactions on Pattern Analysis and Machine Intelligence*, 12, 629-639.

[7] Alvarez, L., Lions, P.L., Morel, J. (1992). Image selective smoothing and edge detection by nonlinear diffusion. II. *SIAM Journal on Numerical Analysis*, 29 (3), 845-866.

[8] Anagaw, A.Y., Sacchi, M.D. (2012). Edge-preserving seismic imaging using the total variation method. *Journal of Geophysics and Engineering*, 9, 138-146.

[9] Barbu, T. (2014). Robust anisotropic diffusion scheme for image noise removal. *Procedia Computer Science*, 35, 522-530.

[10] Barbu, T. (2015). Nonlinear PDE model for image restoration using second-order hyperbolic equations. *Numerical Functional Analysis and Optimization*, 36, 1375-1387.

[11] Droske, M., Bertozzi, A.L. (2010). Higher-order feature-preserving geometric regularization. *SIAM Journal on Imaging Sciences*, 3, 21-51.

[12] Gerig, G., Kubler, O., Kikinis, R., Jolesz, F.A. (1992). Nonlinear anisotropic filtering of MRI data. *IEEE Transactions on Medical Imaging*, 11, 221-232.

[13] Liang, Z., Liu, W., Yao, R. (2016). Contrast enhancement by nonlinear diffusion filtering. *IEEE Transactions on Image Processing*, 25, 673-686.

[14] Oussous, M.A., Alaa, N., Khouya, Y.A. (2014). Anisotropic and nonlinear diffusion applied to image enhancement and edge detection. *Journal of Computer Applications in Technology*, 49, 122-133.

[15] Yu, J., Wang, Y. (2011). Image noise reduction based on anisotropic diffusion: A survey. *Journal of Electronic Measurement and Instrument*, 25, 105-116.

[16] Michelgonzalez, E., Cho, M.H., Lee, S.Y. (2011). Geometric nonlinear diffusion filter and its application to X-ray imaging. *Biomedical Engineering Online*, 10, 47-47.

[17] Ma, W., You, Y., Kaveh, M. (2009). Image restoration regularized by a fourth order PDE. *Proceedings of SPIE*, 724509.

[18] You, Y., Kaveh, M. (2000). Fourth-order partial differential equations for noise removal. *IEEE Transactions on Image Processing*, 9, 1723-1730.

[19] Weickert, J. (1997). A review of nonlinear diffusion filtering. In *Scale-Space Theory in Computer Vision*. LNCS 1252, 1-28.

[20] Youssef, K., Jarenwattananon, N.N., Bouchard, L. (2015). Feature-preserving noise removal. *IEEE Transactions on Medical Imaging*, 34, 1822-1829.

[21] Qiu, Z., Yang, L., Lu, W. (2011). A new feature-preserving nonlinear anisotropic diffusion method for image denoising. In *BMVC 2011: The 22nd British Machine Vision Conference.* BMVA, 1-11.

[22] Li, Y., Jiang, M. (2018). Spatial-fractional order diffusion filtering. *Journal of Mathematical Chemistry*, 56, 257-267.

[23] Zhou, Q., Gao, J., Wang, Z., Li, K. (2016). Adaptive variable time fractional anisotropic diffusion filtering for seismic data noise attenuation. IEEE *Transactions on Geoscience and Remote Sensing*, 54, 1905-1917.

[24] Li, Y., Liu, F., Turner, I.W., Li, T. (2018). Time-fractional diffusion equation for signal smoothing. *Applied Mathematics and Computation*, 326, 108-116.

[25] Cuesta, E., Kirane, M., Malik, S.A. (2012). Image structure preserving denoising using generalized fractional time integrals. *Signal Processing*, 92, 553-563.

[26] Bai, J., Feng, X. (2007). Fractional-order anisotropic diffusion for image denoising. *IEEE Transactions on Image Processing*, 16, 2492-2502.

[27] Janev, M., Pilipovic, S., Atanackovic, T.M., Obradovic, R., Ralevic, N.M. (2011). Fully fractional anisotropic diffusion for image denoising. *Mathematical and Computer Modelling*, 54, 729-741.

[28] Meerschaert, M.M., Benson, D.A., Scheffler, H.-P., Baeumer, B. (2002). Stochastic solution of space–time fractional diffusion equations. *Physical Review E*, 65, 1103-1106.

[29] Feng, L.B., Zhuang, P., Liu, F., Turner, I., Gu, Y.T. (2016). Finite element method for space-time fractional diffusion equation. *Numerical Algorithms*, 72, 749-767.

[30] Chen, Z.Q., Meerschaert, M.M., Nane, E. (2012). Space-time fractional diffusion on bounded domains. *Journal of Mathematical Analysis and Applications*, 393 (2), 479-488.

[31] Azerad, P., Bouharguane, A., Crouzet, J. (2012). Simultaneous denoising and enhancement of signals by a fractal conservation law. *Communications in Nonlinear Science and Numerical Simulation*, 17 (2), 867-881.

[32] Chan, R.H., Lanza, A., Morigi, S., Sgallari, F. (2013). An adaptive strategy for the restoration of textured images using fractional order regularization. *Numerical Mathematics: Theory, Methods and Applications*, 6, 276-296.

[33] Savitzky, A., Golay, M.J.E. (1964). Smoothing and differentiation of data by simplified least squares procedures. *Analytical Chemistry*, 36 (8) 1627-1639.

[34] Krishnan, S.R., Seelamantula, C.S. (2013). On the selection of optimum Savitzky-Golay filters. *IEEE Transactions on Signal Processing*, 61 (2) 380-391.

[35] Eilers, P.H.C. (2003). A perfect smoother. *Analytical Chemistry*, 75, 3631-3636.

[36] Stickel, J.J. (2010). Data smoothing and numerical differentiation by a regularization method. *Computers & Chemical Engineering*, 34, 467-475.

[37] Yandell, B.S. (1989). Spline smoothing and nonparametric regression. *Technometrics*, 31, 379-380.

[38] Liu, B., Sera, Y., Matsubara, N., Otsuka, K., Terabe, S. (2003). Signal denoising and baseline correction by discrete wavelet transform for microchip capillary electrophoresis. *Electrophoresis*, 24 (18), 3260-3265.

[39] Alsberg, B.K., Woodward, A.M., Winson, M.K., Rowland, J.J., Kell, D.B. (1997). Wavelet denoising of infrared spectra. *Analyst*, 122, 645-652.

[40] Yang, Q., Turner, I., Liu, F., Ilic, M. (2011). Novel numerical methods for solving the time-space fractional diffusion equation in two dimensions. *SIAM Journal on Scientific Computing*, 33, 1159-1180.

[41] Momani, S., Odibat, Z. (2008). Numerical solutions of the space-time fractional advection-dispersion equation. *Numerical Methods for Partial Differential Equations*, 24 (6), 1416-1429.

[42] Guan, Q., Gunzburger, M. (2015). θ schemes for finite element discretization of the space-time fractional diffusion equations. *Journal of Computational and Applied Mathematics*, 288, 264-273.

[43] Zhao, J., Xiao, J., Xu, Y. (2013). A finite element method for the multiterm time-space Riesz fractional advection-diffusion equations in finite domain. *Abstract and Applied Analysis*, 2013, 1-15.

[44] Latifizadeh, H. (2010). Analytical solution of linear and non-linear space-time fractional reaction-diffusion equations. *International Journal of Chemical Reactor Engineering*, 8 (1).

Received September 30, 2020
Accepted February 09, 2021